Geoderma 319 (2018) 80–88

Contents lists available at ScienceDirect

Geoderma

journal homepage: www.elsevier.com/locate/geoderma

# Effects of cover crop and biofuel crop management on computed tomography-measured pore parameters

Melis Cercioglu[a,*], Stephen H. Anderson[b], Ranjith P. Udawatta[b,c], Samuel I. Haruna[d]

[a] Dumlupinar University, Vocational College of Simav, Simav 43500, Kutahya, Turkey
[b] School of Natural Resources, University of Missouri, Columbia, MO 65211, USA
[c] The Center of Agroforestry, School of Natural Resources, University of Missouri, Columbia, MO 65211, USA
[d] School of Agribusiness and Agriscience, Middle Tennessee State University, Murfreesboro, TN 37132, USA

ARTICLE INFO

Handling Editor: Morgan Cristine L.S.

*Keywords:*
Cover crop
Image analysis
Miscanthus
Soil pores
Switchgrass

ABSTRACT

Understanding the effects of cropping practices on soil pore characteristics is important for determining soil productivity and ecosystem services. Objectives of the study were to compare differences in computed tomography (CT) measured soil pore parameters (number of macropores, macroporosity, area of the largest pore, circularity and fractal dimension) among cover crops (CC), no-cover crops (NCC), and biofuel crops [Miscanthus (M): *Miscanthus x giganteus* and switchgrass (SG): *Panicum virgatum*] and examine relationships between CT-measured pore parameters and soil hydraulic and thermal properties. Cover crops were Cereal rye (*Secale cereale* L.), Hairy vetch (*Vicia villosa*) and Austrian winter pea (*Pisum sativum* subsp. *arvense*). Three replicates each of undisturbed soil cores were collected at two soil depths (0–10 and 10–20 cm) from each treatment using plexiglass cores measuring 76.2 mm diameter by 76.2 mm long. Ten scan images from each core were acquired using an X-ray CT scanner with 0.19 by 0.19 mm pixel resolution with 0.5 mm slice thickness and analyzed with *Image-J*. Soil under CC, NCC, M, and SG on average had 21, 14, 17, and 12 macropores on a 2500 $mm^2$ area across all the depths. Soil under miscanthus had significantly greater macroporosity (0.049 $m^2\ m^{-2}$) and area for the largest pore (89.70 $mm^2$) than other treatments. The cover crop treatment had approximately 50%, 28%, and 75% greater number of macropores than NCC, M, and SG treatments. Bulk density ($D_b$) of soil was 13% lower in M than the NCC. Saturated hydraulic conductivity ($K_{sat}$) values were positively correlated with most CT-measured pore parameters. In contrast, $D_b$ was negatively correlated with most CT-measured pore parameters (circularity and fractal dimension were positively correlated). While the circularity values were correlated positively with $D_b$ and thermal conductivity ($\lambda$), the fractal dimension was correlated positively with volumetric heat capacity ($C_v$). The study illustrates that M and CC treatments can improve soil pore parameters.

## 1. Introduction

Fluid and gas transmission and storage depend on the geometry and size distribution of soil pores (Eynard et al., 2004). The soil pore network, especially the pore size distribution and connectivity of the pores, is believed to control soil hydraulic properties (Perret et al., 2000; Pierret et al., 2002; Vogel, 2000). Macropores allow rapid preferential (i.e. non-equilibrium) flow of water, dissolved solutes and particulate matter to subsurface and deeper soil horizons. However, excessive flow with contaminants potentially causes serious water quality issues (Jarvis, 2007).

Various soil and crop management practices can influence soil pore parameters. Examples of such management practices include cover crop usage and biofuel cultivation. Cover crops are defined as "crops grown primarily for the purpose of protecting and improving soil between periods of regular crop production" (Schnepf and Cox, 2006). Cover crops have long been valued for their soil conservation benefits, including reducing erosion, increasing infiltration, and improving soil health (Chatterjee, 2013; Kaspar et al., 2001; Kaspar and Singer, 2011; Schnepf and Cox, 2006). The introduction of cover crops within the crop rotation cycle is a widely used measure to improve soil quality and fertility. Most cover crops are grown in periods when the field is left bare to help prime the soil for the corresponding cash crops (Yunusa and Newton, 2003) by influencing soil physical and hydraulic properties.

Because of the necessity for alternative energy production,

*Abbreviations:* CC, cover crop; CT, computed tomography; M, miscanthus; NCC, no-cover crop; PB, perennial biofuel crops; SG, switchgrass

* Corresponding author.
*E-mail address:* melis.cercioglu@dpu.edu.tr (M. Cercioglu).

https://doi.org/10.1016/j.geoderma.2018.01.005
Received 1 September 2017; Received in revised form 16 December 2017; Accepted 4 January 2018
Available online 10 January 2018
0016-7061/ 

perennial biofuel crops like miscanthus (*Miscanthus x giganteus*) and switchgrass (*Panicum virgatum*) are being grown for conversion to biofuel (Gressel, 2008). Due to their year-round surface cover, these perennial crops may protect soil from erosion, improve soil properties, water retention, soil productivity, and wildlife habitat and diversity (Blanco-Canqui et al., 2011). Roots and earthworm burrows under perennial biofuel crops can penetrate compacted soil layers and alter the pore structure, increasing water infiltration and storage at lower depths (Katsvairo et al., 2007). Thus, management practices greatly influence soil hydraulic properties and soil pore parameters and these parameters can be analyzed in the laboratory.

In order to examine the hydraulic properties of soil, non-invasive measurements of soil structure are required. Various properties of soil macropores and macropore networks have been estimated by X-ray CT imagery: porosity (Rachman et al., 2005; Udawatta et al., 2006, 2008a, 2008b; Udawatta and Anderson, 2008), solute movement (Anderson et al., 2003), pore continuity (Pierret et al., 2002), fractal dimension of porosity (Gantzer and Anderson, 2002), and plant root development (Tracy et al., 2010). In recent studies, Rachman et al. (2005), Udawatta et al. (2006, 2008a, 2008b) and Udawatta and Anderson (2008) used X-ray CT to delineate soils under row crop, no-till, and perennial buffers using macropore parameters. They observed strong correlations between macropores estimated using water retention and CT procedures. Macropore characteristics such as shape, size, orientation, and size distribution affect the rate, flow, and retention of water (Anderson, 2014; Udawatta et al., 2013).

There has been significant growth in the use of X-ray CT-measured pore parameters to quantify water flow in soil non-destructively (Mooney, 2002; Mooney et al., 2012). Mathematical modelling combined with CT has also been widely used to obtain properties of porous materials based on pore scale geometries (Blunt et al., 2013). Recently, Tracy et al. (2015) combined CT imaging and image based quantification with numerical modelling (Daly and Roose, 2014; Pavliotis and Stuart, 2008) to calculate the hydraulic conductivity of soil using direct measurements of soil pore structure under a range of different saturation conditions.

Despite the increased growth in the use of X-ray CT in quantifying soil pore parameters resulting from management practices such as tillage, such studies are limited on pore parameters generated by cover and perennial biofuel crops. The objective of the study was to compare differences in CT-measured pore properties (number of macropores, macroporosity, area of the largest pore, circularity and fractal dimension) as affected by cover crop and perennial biofuel crops and correlate these CT-measured pore parameters with soil hydraulic and thermal properties. This study will provide improved understanding of the influence of cover crops and perennial biofuel crops on fluid and gas transmission and storage within the soil.

## 2. Materials and methods

### 2.1. Experimental site

This study was carried out at the University of Missouri Bradford Research Center, which is located about 18 km east of Columbia. The soil was classified by the United States Department of Agriculture (USDA) as Mexico silt-loam (fine, smectitic, mesic Vertic Epiaqualfs) (Table 1). The study site was in a 50 yr corn (*Zea mays* L.)-soybean (*Glycine* max L.) rotation with moldboard plow prior to the establishment of this research. The experiment was laid out in a completely randomized design with three replications each of cover crops, at two levels (cover crop, CC; no-cover crop, NCC), and two levels of perennial biofuel crops (PB). The cover crop mixture consisted of Cereal rye (*Secale cereale* L.), Hairy vetch (*Vicia villosa*) and Austrian winter pea (*Pisum sativum* subsp. *arvense*). The main crop grown on the field was corn (*Zea mays* L.), planted in May and harvested in September of each growing season and the soil was under no tillage management. The perennial biofuel crops were miscanthus (M) (*Miscanthus x giganteus*) and switchgrass (SG) (*Panicum virgatum*), both referred to as perennial biofuel crops.

**Table 1**
Soil physical and chemical properties for the University of Missouri Bradford Research Center study site (Mexico silt loam).

| Soil depth | Soil horizon | Sand | Silt | Clay | SOC |
|---|---|---|---|---|---|
| (cm) | | (%) | | | (g kg$^{-1}$) |
| 0–10 | Ap | 5.4 | 75.9 | 18.7 | 17.2 |
| 10–20 | Ap | 4.8 | 77.2 | 18.0 | 12.2 |

SOC: soil organic carbon.

The cover crop plots were established in 2010 and they were seeded each year in September and October, allowed to grow throughout the winter months, and then terminated in late spring of the following year. The cover crop for this research study was over-seeded on September 8, 2014 and then drilled in on October 1, 2014 at the following rates; Cereal rye (50 kg ha$^{-1}$), Hairy vetch (17 kg ha$^{-1}$) and Austrian winter pea (34 kg ha$^{-1}$) using a Kinze® 38 cm row planter with special blades that allowed small seeded cover crop to be planted. The cover crop was allowed to grow during the winter months and terminated in June using glyphosate (*n*-[*phosphonomethyl*]*glycine*). The perennial biofuel crops were established in 2007. Miscanthus seedlings were hand planted (plugs) in a 0.9 × 0.9 m grid (1984 plants ha$^{-1}$). Switchgrass was planted using a Tye Drill in 19 cm spacing at 7 kg seeds ha$^{-1}$. The perennial biofuel crops were harvested with a silage chopper every year and the biomass was removed and used for biofuel production. All plots were rain-fed during this study.

### 2.2. Sampling and preparation

Soil samples were removed vertically from nontrafficked row areas using a sampler (Uhland, 1950) with Plexiglas cylinders measuring 76.2 mm diameter by 76.2 mm long in early June 2015. These samples were collected one week before the cover crop termination from each of the aforementioned treatments and replicates from two depths, 0–10 and 10–20 cm (4 treatments × 2 depths × 3 replicates = 24 cores). Two plastic caps and masking tape were used on each end of the sample to secure soil inside the cylinders. The soil samples were trimmed in the field, labeled, and sealed in plastic bags and then transported to the laboratory. All soil samples were stored in a cold storage room at 4 °C until analysis was performed.

After the soil cores were removed from the cold storage, the plastic cap on the bottom was removed. The bottom end of the cores was covered with two layers of fine nylon mesh to secure soil within the cylinder and the top plastic cap was removed. The soil cores were slowly saturated from the bottom with distilled water using a Mariotte system. After 24 h saturation period, wet weights were recorded and samples were placed on a 3.5 kPa glass-bead tension table and left to drain for 24 h. This procedure removed water from macropores to enhance the image contrast between air-filled pores and soil solids. Samples were re-weighed and secured with two plastic end caps using masking tape, and then refrigerated prior to scanning. The samples were then taken out from refrigerator and weighed again and prepared (put into the wooden box container) for transport to the University of Missouri Veterinary Medicine Hospital for computed tomography (CT) measurement. A distilled water phantom (in an aluminum tube, outside and inside diam. 2.32 and 1.60 mm) and a solid copper wire phantom (outside diam. 0.55 mm) were attached to the long axis of the Plexiglas cylinder for a standard comparison of values through scans.

### 2.3. Scanning and image analysis

A Toshiba Aquilion 64 X-ray CT scanner set at a peak voltage of

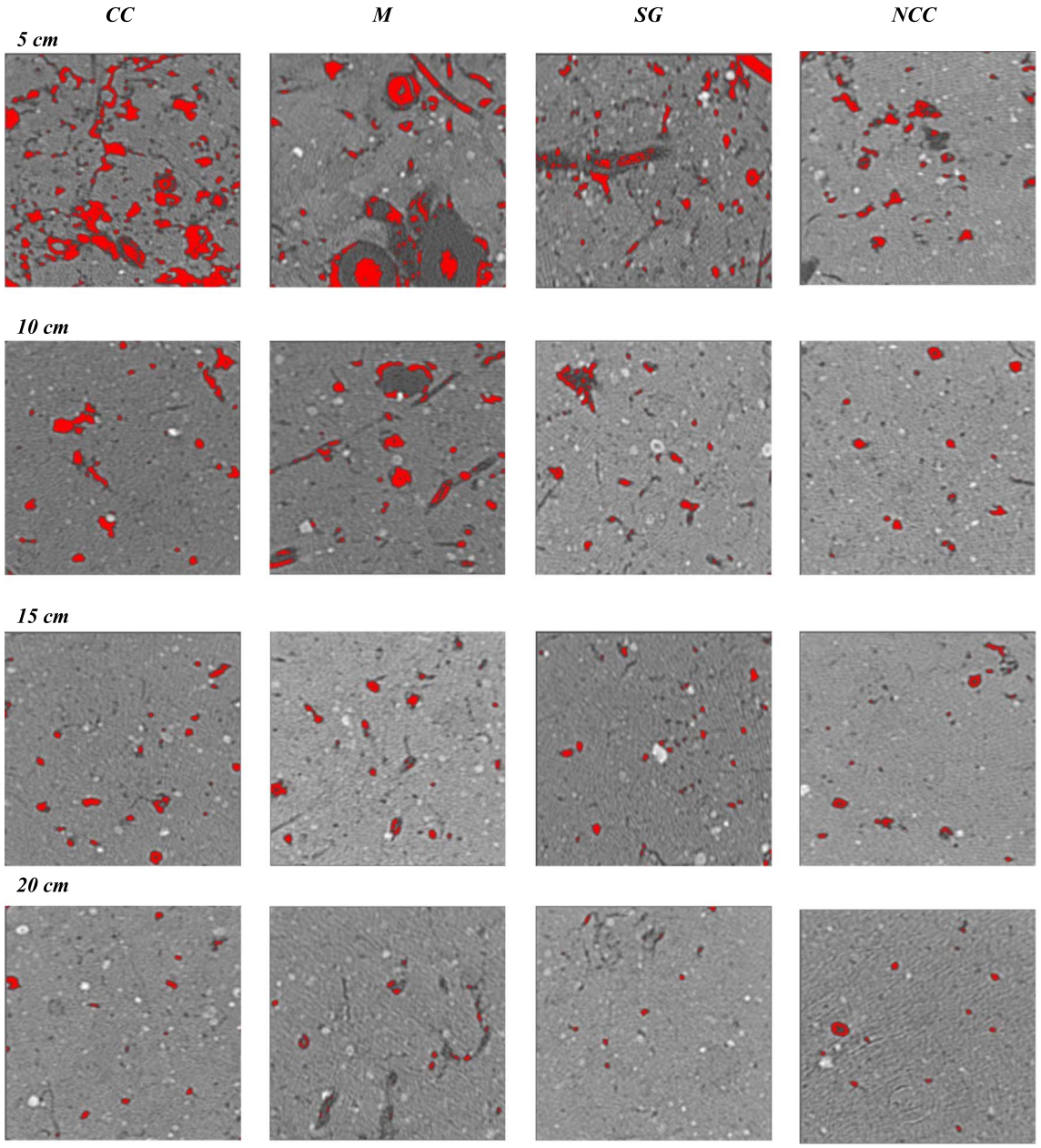


**Fig. 1.** CT scan images of cover crop (CC), miscanthus (M), switchgrass (SG), and no-cover crop (NCC) treatments for four scan depths in a selected profile. The air-filled pores are shown in red, water-filled and root-filled pores in darker gray, soil matrix in lighter gray, and iron and manganese concentrations in white. (For interpretation of the references to colour in this figure legend, the reader is referred to the web version of this article.)

120 keV and a current of 100 mA was used to acquire images. Soil samples were placed horizontally on the scanner bench so that the X-ray beam was perpendicular to the longitudinal axis. The scanning produced images with a slice thickness of 0.5 mm with a pixel size of 0.19 by 0.19 mm. Ten scan slices per sample were taken. A total of 240 images were analyzed within the 20 cm depth using the *Image-J* version 1.50i software (Rasband, 2013) to classify pores into macropores (> 1000 μm diam.) (Zaibon et al., 2016). The Threshold tool was used to distinguish pores from solids after converting the image into an 8-bit grayscale image. A value of 60 was selected as the threshold value to analyze all images. The values lower than 60 were identified as the air-filled pores and values > 60 were identified as non-pore (Fig. 1). Number of macropores, pore area, pore perimeter, circularity and macroporosity statistics were obtained from Analyze Particles Tool. To calculate macroporosity of an image, the macropore area was divided by the 2500 $mm^2$ area. Pore circularity ($C$) values were estimated using the following equation:

$$C = \frac{4\pi(Ap)}{(Pp)^2} \quad (1)$$

where $Ap$ is the pore area and $Pp$ is the pore perimeter (Tuller and Or, 2001). The fractal dimension of pores in images (option in *Image-J*) was estimated with 100 as the threshold value. A different threshold value was used (100 vs. 60) to better populate the low porosity samples with pores and allow computation of the fractal dimension (Gantzer and Anderson, 2002).

### 2.4. Saturated hydraulic conductivity and bulk density

After the scanning procedure, the saturated hydraulic conductivity ($K_{sat}$) and bulk density ($D_b$) were determined on all soil samples. These samples were covered with cheese-cloth at the bottom and saturated in

a 15-cm depth plastic tray with tap water (Electrical conductivity = 0.68 dS $m^{-1}$; Sodium absorption ratio = 2.34) before $K_{sat}$ was measured. The constant-head method was used for $K_{sat}$ determination and the falling head method was used on some samples with very low $K_{sat}$ values (Reynolds and Elrick, 2002). After saturation, the samples were weighed, placed on pressure plates, and equilibrated to − 33, − 100, and − 300 kPa (Dane and Hopmans, 2002) of pressure in a temperature-controlled room (25 °C) for measurement of thermal properties. The soils were equilibrated for 120 h at each pressure. The soils were weighed after equilibration at each pressure and water content was determined at each of those pressures. The samples were air-dried and weighed. After thermal properties were measured, a subsample was dried at 105 °C until a constant weight was obtained. Bulk density ($D_b$) measurements were performed as described by Grossman and Reinsch (2002). The $K_{sat}$ and $D_b$ values were also correlated with CT-measured pore parameters using regression equations.

### 2.5. Thermal properties

Soil thermal properties (thermal conductivity and volumetric heat capacity) were measured using a KD2 (Decagon Devices, Pullman, WA) dual-probe heat-pulse sensor (Haruna et al., 2017). The probe was calibrated before measurement and its accuracy was tested using performance verification standards. Soil core samples were equilibrated on ceramic plates in pressure chambers at four selected water pressures prior to measurement of thermal properties (0, − 33, − 100, and − 300 kPa). The heat pulse probe was inserted vertically into the soil and thermal properties were recorded at each pressure (0, − 33, − 100, and − 300 kPa). Triplicate measurements were made for each core sample. Care was taken to ensure proper contact between the soil and the probes as improper contact can lead to errors in measurement (Abu-Hamdeh et al., 2001). This was done by inserting the probe into new areas during each measurement and also avoiding core walls. Thermal conductivity and volumetric heat capacity were measured for each sample. Also, these properties were correlated with CT-measured pore parameters.

### 2.6. Statistical analysis

A test of variance homogeneity within the different treatments was performed to examine the variability in the measurements. Analysis of variance (ANOVA) was conducted using the PROC GLM procedure with SAS 9.4 (SAS Institute, 2015). Means and differences among means for the measured parameters were determined with PROC MEANS. Least significant differences (Duncan's LSD) were used to assess significant differences among the treatments at the 95% probability level at each soil depth zone 10, and 20 cm. Contrasts among treatments were determined to find significant differences among management practices. PROC CORR procedure was used to determine initial relationships between thermal conductivity, thermal heat capacity, $K_{sat}$, and $D_b$ with the CT-measured pore parameters. The stepwise regression procedure was used to estimate the best relationship using the CT-measured pore parameters in predicting the physical properties.

## 3. Results and discussion

### 3.1. CT-measured number of macropores and macroporosity

Two terms (depth zone and scan depth) were used to distinguish between the two depth zones or soil core depths (0–10 cm, and 10–20 cm) and the 20 scan depths (ten scans per depth zone), respectively, to explain CT-measured pore parameters. The ANOVA results indicated that the pore size distribution varied among the treatments and depth zones studied and significant ($P < .05$) differences were found between some of the treatments and soil depth zones and also some interactions (Table 2). Averaged across the two depth zones, CC, NCC, M, and SG treatments had 21, 14, 17, and 12 macropores on a 2500 $mm^2$ scan area, respectively (Table 2). There were no significant ($P < .05$) differences between the M and NCC treatments. Soil under CC treatment had significantly ($P < .05$) more macropores than the other treatments. In the CC treatment, number of macropores decreased from 53 at the 1 cm depth to 6 at the 20 cm depth (Fig. 2a). The greater number of macropores in the CC treatment may imply water quality benefits including reduced surface nutrient losses and runoff volumes (Cadisch et al., 2004). Also, a greater number of pores usually indicates a higher level of macroporosity since most of the detected pores with the scanner for this study are in the macropore range (> 1000 μm). These pores allow higher rates of water transmission when pores are water-filled or higher rates of gas transmission when pores are air-filled (Kim et al., 2010).

Generally, number of macropores decreased with increasing soil depth zone for all the treatments ($P < .05$, Table 2). The decrease in pores by depths could be attributed to more organic matter accumulation and better root activity in the soil surface horizons as reported by Haruna et al. (2017) under similar management. Longevity of roots and a longer growing season may have increased number of pores in the soil under permanent vegetation as compared with the crop areas (Bharati et al., 2002; Rachman et al., 2005). Literature shows that soils under perennial vegetation have more pores than agricultural areas due to more roots and organic matter and less disturbance (Seobi et al., 2005; Udawatta et al., 2006).

CT-measured macroporosity decreased with increasing depth zones for all the treatments (Fig. 2b). The study by Jiang et al. (2007) agreed with these results; they found that macroporosity decreased with sampling depth at the footslope and backslope positions as a result of higher clay content at deeper soil depths. Macroporosity values averaged across all scan depths were 0.038, 0.016, 0.049, and 0.026 $m^2\ m^{-2}$ for CC, NCC, M, and SG, respectively (Table 2). The macroporosity values were significantly ($P < .05$) greater (206%) in the M treatment when compared to the NCC treatment (Table 2).

### 3.2. CT-measured circularity and largest pore area

Pore circularity is a measure of the shape of the macropores; higher values of circularity indicate that pores are more circular. If the pore is a perfect circle, the circularity is 1.0. If two pore areas are similar, then the pore with a more irregular surface will have a higher measured perimeter and a lower circularity value. The circularity was significantly affected by all the treatments ($P < .05$, Table 2, Fig. 3a) and the average varied between 0.460 and 0.552 (Table 2). Averaged circularity values were found to be significantly ($P < .05$) higher in CC treatment and increased by soil depth zone from 0.482 to 0.581 (Table 2). The M treatment showed greater circularity values (0.669) at the second depth zone than the other treatments (Fig. 3a). Our findings support previous research by Kumar et al. (2010) and Udawatta et al. (2008a) relative to perennial vegetative treatment effects on this parameter.

Since solute and water transport in soils are significantly influenced by size, shape, and distribution of pores and the largest pore size, we have examined pore parameters of the largest pore within each scan. The area of largest pore was significantly different among all the treatments ($P < .05$, Table 2, Fig. 3b). Miscanthus treatment had the largest pore area (89.70 $mm^2$), followed by the SG (43.06 $mm^2$) and CC (27.53 $mm^2$) treatments. Also, miscanthus treatment had about 8 times higher area of largest pore than the NCC (10.89 $mm^2$) treatment (Table 2). Within the first depth zone, the M treatment had a larger pore area (260.03 $mm^2$) when compared to the other treatments (Fig. 3b). Study results indicate the effects of soil disturbance on pores as PB had the largest pores where disturbance is minimal. Similarly, Lipiec and Hatano (2003) reported that management practices mostly affect the number and area of large elongated pores. Larger pores allow rapid drainage of water after heavy rain (Scott, 2000) and may help decrease

**Table 2**
CT-measured pore parameters for cover crop (CC), no-cover crop (NCC), miscanthus (M), switchgrass (SG), row crops (RC, include CC and NCC) and perennial biofuel (PB, include M and SG) crops and by depth along with the ANOVA.

| | Number of macropores | Macroporosity ($m^2\ m^{-2}$) | Area of largest pore ($mm^2$) | Circularity | Fractal dimension |
|---|---|---|---|---|---|
| *Treatment means* | | | | | |
| CC | 21 a | 0.038 ab | 27.53 ab | 0.552 a | 1.877 a |
| NCC | 14 ab | 0.016 b | 10.89 b | 0.513 ab | 1.706 a |
| M | 17 ab | 0.049 a | 89.70 a | 0.477 b | 1.850 a |
| SG | 12 b | 0.026 ab | 43.06 ab | 0.460 b | 1.786 a |
| *Depth zone means* | | | | | |
| 0–10 cm | 23 a | 0.056 a | 78.12 a | 0.482 b | 1.817 a |
| 10–20 cm | 8 b | 0.009 b | 7.47 b | 0.581 a | 1.793 b |
| *Treatment × depth* | | | | | |
| CC × 0–10 cm | 33 a | 0.068 a | 46.88 ab | 0.547 a | 1.917 a |
| CC × 10–20 cm | 9 cd | 0.009 c | 8.18 b | 0.559 a | 1.838 a |
| NCC × 0–10 cm | 20 abc | 0.025 bc | 13.71 b | 0.502 a | 1.746 a |
| NCC × 10–20 cm | 8 cd | 0.009 c | 8.08 b | 0.524 a | 1.666 a |
| M × 0–10 cm | 23 ab | 0.086 a | 170.08 a | 0.439 a | 1.789 a |
| M × 10–20 cm | 10 bcd | 0.012 c | 9.31 b | 0.516 a | 1.912 a |
| SG × 0–10 cm | 17 bcd | 0.046 abc | 81.80 ab | 0.438 a | 1.818 a |
| SG × 10–20 cm | 6 d | 0.006 c | 4.33 b | 0.483 a | 1.756 a |
| *Analysis of variance P > F* | | | | | |
| Treatment | 0.069 | 0.079 | 0.111 | 0.034 | 0.152 |
| RC vs. PB | 0.145 | 0.237 | 0.049 | 0.009 | 0.607 |
| CC vs. NCC | 0.045 | 0.085 | 0.580 | 0.171 | 0.042 |
| M vs. SG | 0.172 | 0.070 | 0.145 | 0.534 | 0.395 |
| Scan depth | < 0.001 | < 0.001 | < 0.001 | 0.002 | 0.049 |
| Treatment by scan depth | 0.149 | 0.337 | 0.016 | 0.371 | 0.765 |

The ANOVA table presents significance levels among treatments and by depth for the measured parameters. Within columns, values followed by the same letter for the treatments or the depths are not significantly different at the .05 probability level.

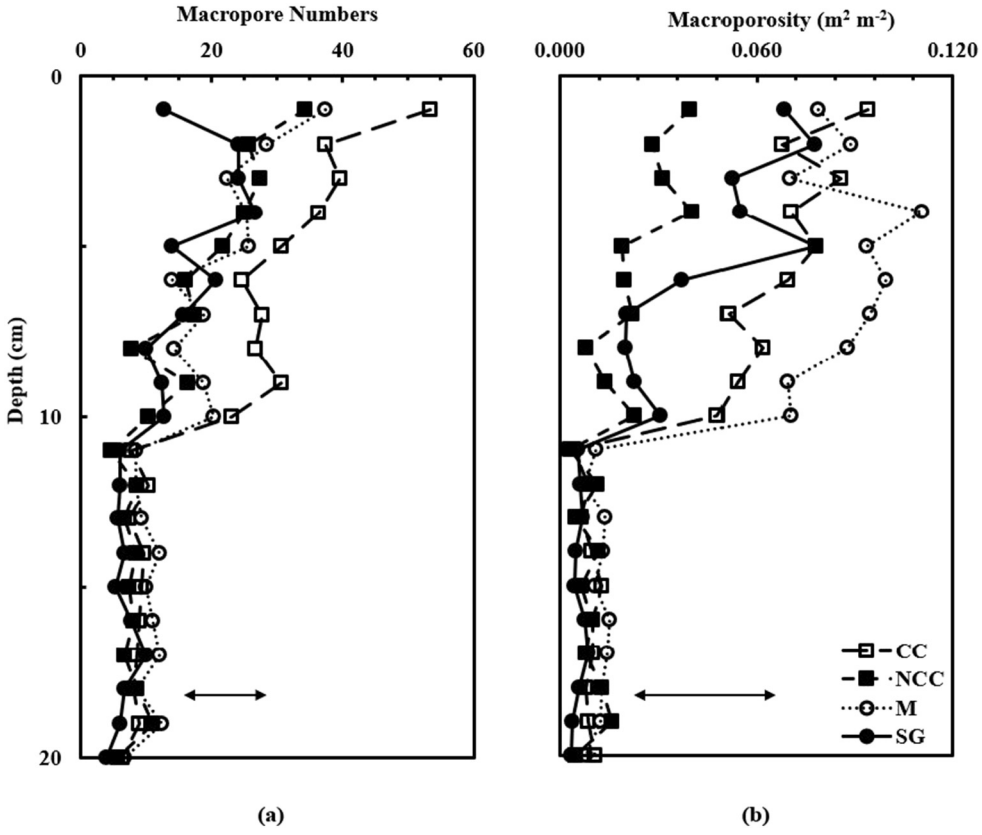


**Fig. 2.** CT-measured (a) number of macropores and (b) macroporosity for cover crop (CC), miscanthus (M), switchgrass (SG), and no-cover crop (NCC) treatments influenced by depth (n = 20). The bar indicates the LSD (0.05) values.

runoff.

Improvement in soil pore parameters is beneficial, both agronomically and environmentally. Results from the current study indicates that CC, when included into crop production cycles, can help improve soil ecosystem services. This can also help reduce nutrient loading into streams and reduce the incidence of hypoxia in rivers, oceans and estuaries around the world. Perennial biofuel crops can also provide these benefits. In addition, CC and PB can increase soil organic carbon (Haruna et al., 2017), thus increasing carbon sequestration. Therefore, these crops could become more important in a more variable global

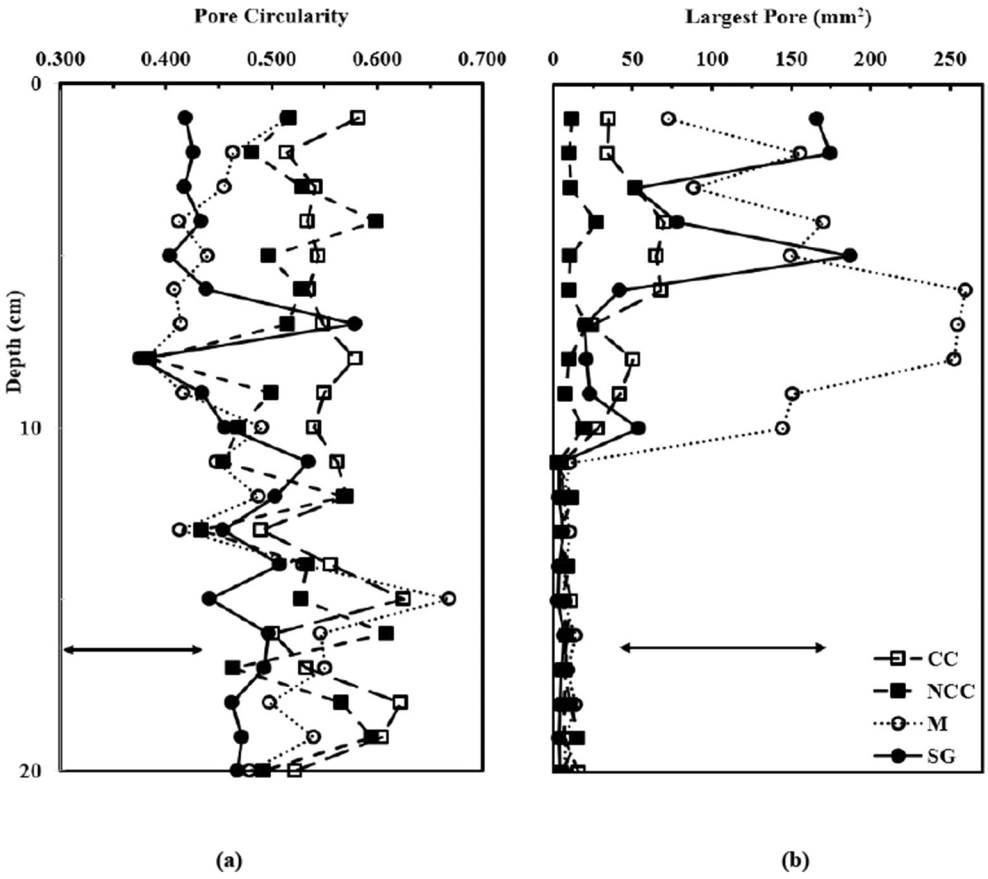


**Fig. 3.** CT-measured (a) pore circularity and (b) area of largest pore for cover crop (CC), miscanthus (M), switchgrass (SG), and no-cover crop (NCC) treatments influenced by depth (n = 20). The bar indicates the LSD (0.05) values.

climate.

### 3.3. CT-measured fractal dimension

Structural properties of a porous media can be explained using fractal dimension (Dathe and Thullner, 2005) and fractal dimension values presented in this section apply to CT-measured macropores. Larger fractal dimension values indicate that the macropores are more space filling in the image. While the fractal dimension of macropores wasn't significantly different among the treatments, this parameter was affected significantly by depth zone (Table 2). The highest numerical value of fractal dimension was observed in the CC (1.877) treatment when compared to other treatments. As previously mentioned, the CC treatment had a greater number of macropores than the other treatments and this may suggest a higher probability of preferential water flow due to large and more elongated pores in the CC treatment as compared with the NCC and M treatments. The fractal dimension decreased from the first to the second depth zone (1.817 to 1.793) across all the treatments as did macroporosity ($P < .05$, Table 2). Decreasing fractal dimension values as a function of soil depth zone as found in the current study has also occurred in other studies (Rachman et al., 2005). A decrease of 1.34% was found for the fractal dimension from the 10 to 20 cm depth zones of the current study, while Rachman et al. (2005) found a decrease of 17% from the 5 to 15 cm soil depth zone. Udawatta and Anderson (2008) reported a 19% decrease in fractal dimension from the 5 to 45 cm soil depth in claypan soils.

### 3.4. Saturated hydraulic conductivity and bulk density

Saturated hydraulic conductivity ($K_{sat}$) and bulk density ($D_b$) means averaged over the two depth zones are given in Table 3. Results showed significant depth zone effects on both $K_{sat}$ and $D_b$ ($P < .05$). The $K_{sat}$ values significantly decreased with increasing depth zone (441 and 39.9 mm $h^{-1}$, respectively) but this parameter was not significantly different across all the treatments.

**Table 3**
Arithmetic mean of bulk density ($D_b$) and geometric mean of saturated hydraulic conductivity ($K_{sat}$) for cover crop (CC), no-cover crop (NCC), miscanthus (M), switchgrass (SG), row crops (RC, include CC and NCC) and perennial biofuel (PB, include M and SG) crops and by depth along with the ANOVA.

| | $D_b$ (g $cm^{-3}$) | $K_{sat}$ (mm $h^{-1}$) |
|---|---|---|
| *Treatment means* | | |
| CC | 1.33 ab | 250 a |
| NCC | 1.38 a | 30.0 a |
| M | 1.22 c | 321 a |
| SG | 1.24 bc | 129 a |
| *Depth zone means* | | |
| 0–10 cm | 1.14 b | 441 a |
| 10–20 cm | 1.44 a | 39.9 b |
| *Analysis of variance P > F* | | |
| Treatment | < 0.001 | 0.161 |
| RC vs. PB | < 0.001 | 0.265 |
| CC vs. NCC | 0.025 | 0.068 |
| M vs. SG | 0.205 | 0.390 |
| Depth zone | < 0.001 | 0.016 |
| Treatment by depth zone | < 0.001 | 0.294 |

Within columns, values followed by the same letter for the treatments or the depths are not significantly different at the .05 probability level.

According to the results, $D_b$ under row crop (RC) treatments (NCC and CC) was 1.35 g $cm^{-3}$, approximately 10% greater than that under PB treatments (M and SG). Results also showed that soil $D_b$ changed (1.22 to 1.38 g $cm^{-3}$) significantly among treatments. The lowest $D_b$ was found under M treatment ($P < .05$, Table 3). Bulk density was

significantly higher in NCC compared to CC management and also increased significantly ($P < .05$) from the first to second soil depth zone.

### 3.5. Correlation of CT-measured pore parameters with hydraulic conductivity and thermal properties

Saturated hydraulic conductivity ($K_{sat}$) was positively correlated with number of macropores (r = 0.69, $P = .0002$), area of the largest pore (r = 0.61, $P = .0015$), and macroporosity (r = 0.74, $P \leq .0001$). Rachman et al. (2005) also reported a positive correlation between $K_{sat}$ and CT-measured macroporosity (r = 0.95). The current study illustrates a good correlation between CT-measured pore parameters and $K_{sat}$. The reason for these relationships is due to the effects of these large pores measured with CT on this water transport property (Kim et al., 2010). Bulk density ($D_b$) was negatively correlated with number of macropores (r = −0.61, $P = .0014$), area of the largest pore (r = −0.73, $P \leq .0001$), and macroporosity (r = −0.78, $P \leq .0001$) while it was positively correlated with circularity (r = 0.57, $P = .0034$).

The CT-measured pore parameters were correlated with soil thermal properties data obtained from Haruna et al. (2017). The CT-measured pore parameter with the best correlation with thermal conductivity (λ) was pore circularity; this result was found to occur for thermal conductivity measured at each soil water pressure. CT-measured circularity was positively correlated (r = 0.36, $P = .787$; r = 0.74, $P \leq .0001$; r = 0.64, $P = .0007$; r = 0.62, $P = .0011$) with λ at all soil water pressures corresponding to 0, −33, −100, and −300 kPa, respectively. The best correlation for λ with CT-measured pore circularity was at −33 kPa (r = 0.74; Fig. 4a). It is speculated that since pore circularity was found to be positivity correlated with $D_b$ for the treatments of this study, the λ will also be positively correlated with CT-measured pore circularity.

Udawatta et al. (2006) reported that 22% more circular pores were found under row crop soils compared to agroforestry buffer and grass buffer soils in Missouri. These row crop soils also had higher bulk density. Adhikari et al. (2014) found the highest thermal conductivity in the row crop soils similar to the current study.

The second best CT-measured pore parameter found to be correlated with λ for all water pressures was area of largest pore. Area of the largest pore was found to be negatively correlated (r = −0.35, $P = .0912$; r = −0.54, $P = .0056$; r = −0.57, $P = .0035$; r = −0.57, $P = .0031$) with λ at soil water pressures corresponding to 0, −33, −100, and −300 kPa, respectively. The best correlation for λ with CT-measured area of largest pore was at −300 kPa (r = −0.57; Fig. 4b). In our study we found that the miscanthus treatment had the highest value for area of the largest pore, the lowest circularity value, and the lowest $D_b$ value compared to the other treatments (Table 2 and Table 3). An increase in $D_b$ of soil, lowers the porosity and improves the thermal contact between soil particles and increases λ (Lal and Shukla, 2004). Haruna et al. (2017) reported that λ was lower under the miscanthus treatment. Some other researchers found that the λ is more strongly correlated with air-filled porosity (difference of saturated and current volumetric water content) than with volume fraction of water (Ochsner et al., 2001; Usowicz et al., 2013).

Of all the CT-measured pore parameters, the one best correlated with volumetric heat capacity ($C_v$) was CT-measured fractal dimension of macropores for all soil water pressures. Fractal dimension was positively correlated (r = 0.45, $P = .0253$; r = 0.43, $P = .0339$; r = 0.47, $P = .0202$; r = 0.52, $P = .0092$) with $C_v$ corresponding to 0, −33, −100, and −300 kPa, water pressures, respectively. The best correlation for $Cv$ with CT-measured fractal dimension was at −300 kPa (r = 0.52; Fig. 4c). Volumetric heat capacity ($C_v$) is strongly related to soil organic carbon (SOC) and water content ($\theta$) (Ju et al., 2011; Ochsner et al., 2001). Since $C_v$ of water and SOC are higher than values of air (Bristow, 2002), the management practices that increase $\theta$ at a given pressure and SOC have the potential to increase $C_v$ (Abu-Hamdeh, 2003). The higher fractal dimension values indicate more macroporosity, a higher amount of soil water retained for a given pressure, and more SOC which all suggest a higher $C_v$.

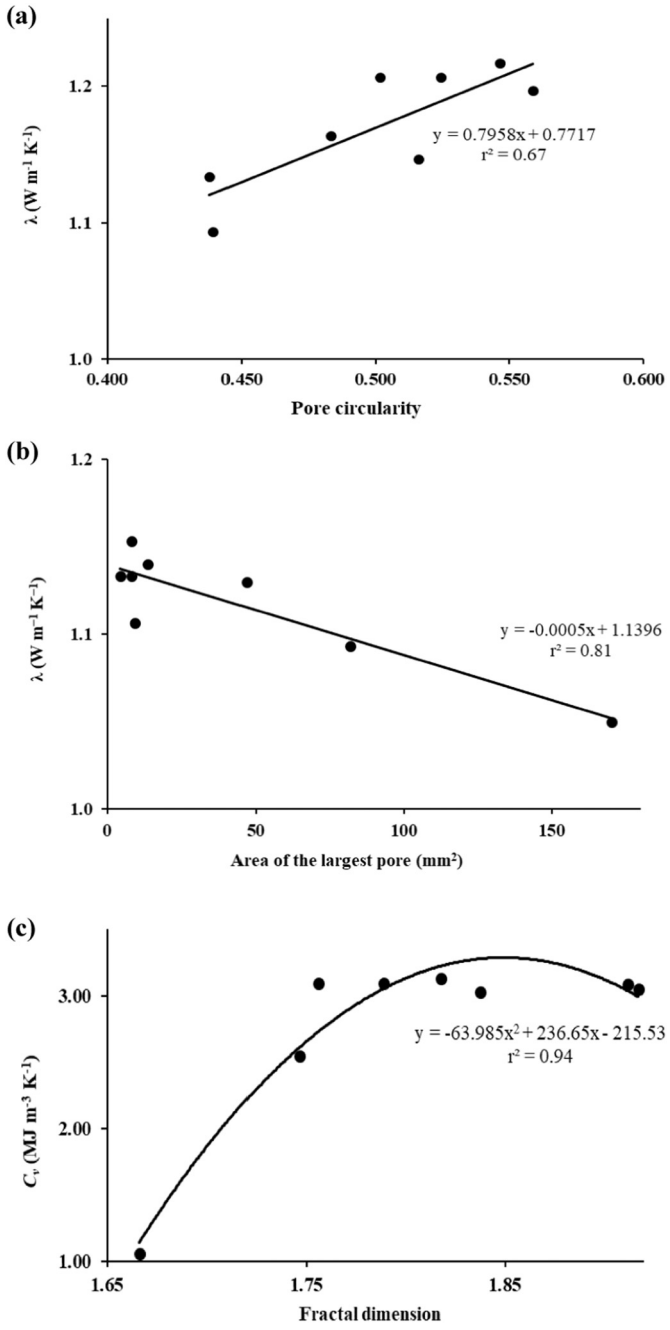


**Fig. 4.** (a) Correlation of thermal conductivity (λ) at −33 kPa soil water pressure and CT-measured pore circularity mean values for all the treatments and sampling depth; (b) correlation of thermal conductivity (λ) at −300 kPa soil water pressure and CT-measured area of largest pore mean values for all the treatments and sampling depth; (c) correlation of volumetric heat capacity ($C_v$) at −300 kPa soil water pressure and CT-measured fractal dimension mean values for all the treatments and sampling depth (Haruna et al., 2017).

Results from the current study showed that cover crops and biofuel crops improved some CT-measured pore parameters. However, more studies are needed in the future to better understand the influence of these management practices on a wider array of soil pore sizes. Such future studies should consider the use of higher resolution scanners and imaging techniques. This will build on the information provided in the current study and help improve understanding on the influence of these management practices on water movement and gas diffusion within the

critical zone.

## 4. Conclusions

This study was conducted to examine changes in CT-measured pore parameters under cover crop, no-cover crop, miscanthus, and switchgrass treatments at two depth zones. Differences were significantly greater for several parameters among treatments in the surface 10 cm depth zone compared with second soil depth zone. CT-measured number of macropores, macroporosity, area of largest pore, and circularity were found to be significantly different among the treatments. Results showed that generally miscanthus and cover crop treatments improved these pore parameters. The miscanthus treatment had significantly higher macroporosity, and area of largest pore, with lower bulk density values than the other three treatments. Increased macroporosity in the miscanthus treatment will probably increase soil water infiltration, increase gas exchange, and decrease runoff and nonpoint-source pollution. The highest number of macropores and circularity were found in the cover crop treatment among all treatments. Furthermore, pore circularity was observed as the best parameter to predict thermal conductivity (positively correlated). Reasons for the relationship of thermal conductivity with pore circularity are probably due to the effects of soil density on pore circularity (higher density is related to higher circularity). The second best parameter for predicting thermal conductivity was area of the largest pore (negatively correlated). The fractal dimension of CT-measured macropores was positively correlated with volumetric heat capacity. Similar to other studies, laboratory-measured saturated hydraulic conductivity was found to be correlated with CT-measured pore parameters; the best parameter was CT-measured macroporosity and was positively correlated with this parameter.

Results show that perennial vegetative treatments and cover crop treatments affect soil pore shapes or forms which are highly correlated with vegetative management. In addition, nondestructive CT techniques prove to be useful to examine pore parameters influenced by crop management to further expand our knowledge on soil pore systems.

As for future directions, more research can be planned for further assessment of pore parameters under cover crop and biofuel management. Efforts utilizing higher resolution scanners to be able to further examine pore size distributions and pore continuity to better assess these management systems.

## Acknowledgments

This work funded through the University of Missouri Center of Agroforestry.

## References

Abu-Hamdeh, N.H., 2003. Thermal properties of soils as affected by density and water content. Biosyst. Eng. 86, 97–102.
Abu-Hamdeh, N.H., Khdair, A.I., Reeder, R.C., 2001. A comparison of two methods used to evaluate thermal conductivity for some soils. Int. J. Heat Mass Transf. 44, 1073–1078.
Adhikari, P., Udawatta, R.P., Anderson, S.H., 2014. Soil thermal properties under prairies, conservation buffers, and corn-soybean land use systems. Soil Sci. Soc. Am. J. 78, 1977–1986.
Anderson, S.H., 2014. Tomography-measured macropore parameters to estimate hydraulic properties of porous media. Procedia Comput. Sci. 36, 649–654.
Anderson, S.H., Wang, H., Peyton, R.L., Gantzer, C.J., 2003. Estimation of porosity and hydraulic conductivity from X-ray CT-measured solute breakthrough. In: Mees, F. (Ed.), Application of X-ray Computed Tomography in the Geosciences. The Geological Society, London, UK, pp. 135–150.
Bharati, L., Lee, K.H., Isenhart, T.M., Schultz, R.C., 2002. Soil-water infiltration under crops, pasture, and established riparian buffer in Midwest USA. Agrofor. Syst. 56, 249–257.
Blanco-Canqui, H., Mikha, M.M., Presley, D.R., Claassen, M.M., 2011. Addition of cover crops enhances no-till potential for improving soil physical properties. Soil Sci. Soc. Am. J. 75, 1471–1478.
Blunt, M.J., Bijeljic, B., Dong, H., Gharbi, O., Iglauer, S., Mostaghimi, P., Paluszny, A., Pentland, C., 2013. Pore-scale imaging and modelling. Adv. Water Resour. 51, 197–216.
Bristow, K.L., 2002. Thermal conductivity. In: Dane, J.H., Topp, G.C. (Eds.), Methods of Soil Analysis. Part 4-Physical Methods. Book Ser. 5. SSSA, Madison, WI, pp. 1209–1226.
Cadisch, G., Willington, P., Suprayogo, D., Mobbs, D.C., Van Noordwijck, M., Rowe, E.C., 2004. Catching and competing for mobile nutrients in soil. In: Van Noordwijk, M. (Ed.), Below Ground Interactions in Tropical Agroecosystems. CABI Publ., Cambridge, MA, pp. 171–192.
Chatterjee, A., 2013. North-Central US: introducing cover crops in the rotation. Crops Soils 46, 14–15.
Daly, K.R., Roose, T., 2014. Multiscale modelling of hydraulic conductivity in vuggy porous media. Proc. R. Soc. London, Ser. A 470, 20130383.
Dane, J.H., Hopmans, J.W., 2002. Water retention and storage. In: Dane, J.H., Topp, G.C. (Eds.), Methods of Soil Analysis. Part 4-Physical Methods. SSSA, Madison, WI, pp. 671–717.
Dathe, A., Thullner, M., 2005. The relationship between fractal properties of solid matrix and pore space in porous media. Geoderma 129, 279–290.
Eynard, A., Schumacher, T.E., Lindstrom, M.J., Malo, D.D., 2004. Porosity and pore-size distribution in cultivated ustolls and usterts. Soil Sci. Soc. Am. J. 68, 1927–1934.
Gantzer, C.J., Anderson, S.H., 2002. Computed tomographic measurement of macroporosity in chisel-disk and no-tillage seedbeds. Soil Tillage Res. 64, 101–111.
Gressel, J., 2008. Transgenics are imperative for biofuel crops. Plant Sci. 174, 246–263.
Grossman, R.B., Reinsch, T.G., 2002. Bulk density and linear extensibility. In: Dane, J.H., Topp, G.C. (Eds.), Methods of Soil Analysis. Part 4-Physical Methods. SSSA Book Ser. 5. pp. 201–228 (Madison, WI).
Haruna, S.I., Anderson, S.H., Nkongolo, N.V., Reinbott, T., Zaibon, S., 2017. Soil thermal properties influenced by perennial biofuel and cover crop management. Soil Sci. Soc. Am. J. 81, 1147–1156.
Jarvis, N.J., 2007. A review of non-equilibrium water flow and solute transport in soil macropores: principles, controlling factors and consequences for water quality. Eur. J. Soil Sci. 58, 523–546.
Jiang, P., Anderson, S.H., Kitchen, N.R., Sadler, E.J., Sudduth, K.A., 2007. Landscape and conservation management effects on hydraulic properties on a claypan-soil toposequence. Soil Sci. Soc. Am. J. 71, 803–811.
Ju, Z., Ren, T., Hu, C., 2011. Soil thermal conductivity as influenced by aggregation at intermediate water contents. Soil Sci. Soc. Am. J. 75, 26–29.
Kaspar, T.C., Singer, J.W., 2011. The use of cover crops to manage soil. In: Hatfield, J.L., Sauer, T.J. (Eds.), Soil Management: Building a Stable Base for Agriculture, pp. 321–337.
Kaspar, T.C., Radke, J.K., Laflen, J.M., 2001. Small grain cover crops and wheel traffic effects on infiltration, runoff, and erosion. J. Soil Water Conserv. 56, 160–164.
Katsvairo, T.W., Wright, D.L., Marois, J.J., Hartzog, D.L., Balkcom, K.B., Wiatrak, P.P., Rich, J.R., 2007. Cotton roots, earthworms, and infiltration characteristics in sod-peanut-cotton cropping systems. Agron. J. 99, 390–398.
Kim, H., Anderson, S.H., Motavalli, P.P., Gantzer, C.J., 2010. Compaction effects on soil macropore geometry and related parameters for an arable field. Geoderma 160, 244–251.
Kumar, S., Anderson, S.H., Udawatta, R.P., 2010. Agroforestry and grass buffer influences on macropores measured by computed tomography under grazed pasture systems. Soil Sci. Soc. Am. J. 74, 203–212.
Lal, R., Shukla, M.R., 2004. Principles of Soil Physics. Marcel Dekker, New York.
Lipiec, J., Hatano, R., 2003. Quantification of compaction effects on soil physical properties and crop growth. Geoderma 116, 107–136.
Mooney, S.J., 2002. Three-dimensional visualization and quantification of soil macroporosity and water flow patterns using computed tomography. Soil Use Manag. 18 (2), 142–151.
Mooney, S.J., Pridmore, T.P., Helliwell, J., Bennett, M.J., 2012. Developing X-ray computed tomography to non-invasively image 3-D root systems architecture in soil. Plant Soil 352, 1–22.
Ochsner, T.E., Horton, R., Ren, T., 2001. A new perspective on soil thermal properties. Soil Sci. Soc. Am. J. 65, 1641–1647.
Pavliotis, G., Stuart, A., 2008. Multiscale Methods: Averaging and Homogenization. Springer, NY.
Perret, J., Prasher, S.O., Kantzas, A., Langford, C., 2000. A two-domain approach using CAT scanning to model solute transport in soil. J. Environ. Qual. 29, 995–1010.
Pierret, A., Capowiez, Y., Belzunces, L., Moran, C.J., 2002. 3D reconstruction and quantification of macropores using X-ray computed tomography and image analysis. Geoderma 106, 247–271.
Rachman, A., Anderson, S.H., Gantzer, C.J., 2005. Computed-tomographic measurement of soil macroporosity parameters as affected by stiff-stemmed grass hedges. Soil Sci. Soc. Am. J. 69, 1609–1616.
Rasband, W., 2013. *Image-J*. National Institutes of Health, Bethesda, MD. https://imagej.nih.gov/ij/, Version 1.50i, Accessed date: 20 April 2017.
Reynolds, W.D., Elrick, D.E., 2002. Saturated and field-saturated water flow parameters: falling head soil core (tank) method. In: Dane, J.H., Topp, G.C. (Eds.), Methods for Soil Analysis. Part 4-Physical Methods. SSSA Book Series. 5. pp. 809–812 (Madison, WI).
SAS Institute, 2015. Base SAS 9.4 Procedures Guide. SAS Institute, Cary, NC.
Schnepf, M., Cox, C., 2006. Environmental Benefits of Conservation on Cropland: The Status of our Knowledge. SWCS, Ankeny, IA.
Scott, H.D., 2000. Soil Physics: Agricultural and Environmental Applications. Iowa State Univ. Press, Ames, Iowa.
Seobi, T., Anderson, S.H., Udawatta, R.P., Gantzer, C.J., 2005. Influence of grass and agroforestry buffer strips on soil hydraulic properties for an albaqualf. Soil Sci. Soc. Am. J. 69, 893–901.
Tracy, S.R., Jeremy, A.R., Black, C.R., McNeill, A., Davidson, R., Mooney, S.J., 2010. The

X-factor: visualizing undisturbed root architecture in soils using X-ray computed tomography. J. Exp. Bot. 61 (2), 311–313.
Tracy, S.R., Daly, K.R., Sturrock, C.J., Crout, N.M.J., Mooney, S.J., Roose, T., 2015. Three-dimensional quantification of soil hydraulic properties using X-ray computed tomography and image-based modeling. Water Resour. Res. 51, 1006–1022.
Tuller, M., Or, D., 2001. Hydraulic conductivity of variably saturated porous media: film and corner flow in angular pore space. Water Resour. Res. 37 (5), 1257–1276.
Udawatta, R.P., Anderson, S.H., 2008. CT-measured pore characteristics of surface and subsurface soils as influenced by agroforestry and grass buffers. Geoderma 145, 381–389.
Udawatta, R.P., Anderson, S.H., Gantzer, J.C., Garrett, H.E., 2006. Agroforestry and grass buffer influence on macropore characteristics: a computed tomography analysis. Soil Sci. Soc. Am. J. 70, 1763–1773.
Udawatta, R.P., Anderson, S.H., Gantzer, J.C., Garrett, H.E., 2008a. Agroforestry and grass buffer effects on pore characteristics measured by high-resolution X-ray computed tomography. Soil Sci. Soc. Am. J. 72, 295–304.
Udawatta, R.P., Anderson, S.H., Gantzer, J.C., Garrett, H.E., 2008b. Influence of prairie restoration on CT-measured soil pore characteristics. J. Environ. Qual. 37, 219–228.
Udawatta, R.P., Anderson, S.H., Gantzer, J.C., Assouline, S., 2013. Computed tomographic evaluation of earth materials with varying resolutions. In: Anderson, S.H., Hopmans, J.W. (Eds.), Soil-Water-Root Processes: Advances in Tomography and Imaging. Part 5. SSSA Special Publication. 61. pp. 97–112 (Madison, WI).
Uhland, R.E., 1950. Physical properties of soils modified by crops and management. Soil Sci. Soc. Am. J. 14, 361–366.
Usowicz, B., Lipiec, J., Usowicz, J.B., Marczewski, W., 2013. Effects of aggregate size on soil thermal conductivity: comparison of measured and model-predicted data. Int. J. Heat Mass Transf. 57 (2), 536–541.
Vogel, H.J., 2000. A numerical experiment on pore size, pore connectivity, water retention, permeability, and solute transport using network models. Eur. J. Soil Sci. 51, 99–105.
Yunusa, I.A.M., Newton, P.J., 2003. Plants for amelioration of subsoil constraints and hydrological control: the primer-plant concept. Plant Soil 257, 261–281.
Zaibon, S., Anderson, S.H., Kitchen, N.R., Haruna, S.I., 2016. Hydraulic properties affected by topsoil thickness in switchgrass and corn–soybean cropping systems. Soil Sci. Soc. Am. J. 80 (5), 1365–1376.